Comparison of Direct Electrocaloric Characterization Methods Exemplified by 0.92 $Pb(Mg_{1/3}Nb_{2/3})O_3$ - 0.08 $PbTiO_3$ Multilayer Ceramics

Christian Molin[1,a], Jani Peräntie[2], Florian Le Goupil[3], Florian Weyland[4], Mehmet Sanlialp[5], Natalie Stingelin[3], Nikola Novak[4], Doru C. Lupascu[5], Sylvia Gebhardt[1]

[1]*Department of Smart Materials and Systems, Fraunhofer Institute for Ceramic Technologies and Systems IKTS, Winterbergstr. 28, 01277, Dresden, Germany*

[2]*Microelectronics Research Unit, University of Oulu, P.O. Box 4500, 90014 Oulu, Finland*

[3]*Department of Materials, Imperial College London, London SW7 2AZ, United Kingdom*

[4]*Institute of Materials Science, Technische Universität Darmstadt, Alarich-Weiss-Straße 2, 64287 Darmstadt, Germany*

[5]*Institute for Materials Science and Center for Nanointegration Duisburg-Essen (CENIDE), University of Duisburg-Essen, Universitätsstrasse 15, 45141, Essen, Germany*

[a]*Corresponding author: E-Mail: christian.molin@ikts.fraunhofer.de*

Electrocaloric device structures have been developed as multilayer ceramics (MLCs) based on fundamental research carried out on PMN-8PT bulk ceramics. Two different MLC structures were prepared with nine layers each and layer thicknesses of 86 µm and 39 µm. The influence of the device design on its properties has been characterized by microstructural, dielectric, ferroelectric, and direct electrocaloric measurement. For direct characterization two different methods, i.e. temperature reading (thermistor and thermocouple) and heat flow measurement (differential scanning calorimetry), were used. A comparison of results revealed a highly satisfactory agreement between the different methods. This study confirms that MLCs are promising candidates for implementation into energy-efficient electrocaloric cooling systems providing large refrigerant volume and high electrocaloric effect (ECE). Due to their micron-sized active layers, they allow for the application of high electric fields under low operation voltages. We measured a maximum electrocaloric temperature change of ΔT = 2.67 K under application/withdrawal of an electric field of ΔE = 16 kV mm^{-1}, which corresponds to operation voltages below 1.5 kV.

I. INTRODUCTION

The electrocaloric effect (ECE), defined as an isothermal entropy or adiabatic temperature change of a dielectric material under application or removal of an electric field,[1] was discovered in 1930.[2] The ECE has gained much scientific interest, when Mischenko et al. reported a giant electrocaloric effect in 2006.[3] Today, different caloric effects, such as magneto-, baro-, and electrocaloric are seen as promising solutions for future solid-state cooling devices, providing highly efficient and environmentally friendly cooling systems.[4] Although magnetocaloric cooling is the most mature technique, it requires the application of huge magnetic fields from expensive rare-earths-containing magnets. ECE cooling on the other hand, uses cheap and readily available materials and has the potential to be significantly more efficient than the current vapor-compression technology.[1] Hence ECE cooling offers an energy-efficient and environmentally-friendly alternative to current cooling technologies, which are already responsible for over 10% of carbon emissions, and could be key to meeting the emission targets set at COP21 in 2015. This study addresses the two main challenges that stifle the progress of ECE cooling: The inability to apply high enough electric fields to bulk materials and the lack of reliable direct measurement reports.

One of the most investigated material system is the relaxor ferroelectric lead magnesium niobate-lead titanate (PMN-PT). It is well known for its good EC properties and shows large EC temperature changes ΔT_{EC} for compositions around the morphotropic phase boundary (30-35% $PbTiO_3$-content).[5,6] However, the maximum electrocaloric effect in morphotropic compositions takes place well above 100 °C. Another well-studied composition is 0.90 $Pb(Mg_{1/3}Nb_{2/3})O_3$-0.10 $PbTiO_3$ which typically shows electrocaloric strengths $\Delta T/\Delta E$ between $0.15 \cdot 10^{-6}$ and $0.24 \cdot 10^{-6}$ K m V^{-1} at temperatures below 100 °C.[7–9]

Here, we consider the composition of 0.92 $Pb(Mg_{1/3}Nb_{2/3})O_3$-0.08 $PbTiO_3$ (PMN-8PT) with a temperature of maximum permittivity T_m around 30 °C and temperature of depolarization well below room temperature[7]. This makes it a suitable material for application in Li-battery cooling at temperatures around 40 °C. PMN-8PT shows the relaxor-typical broad, frequency-dependent peak of permittivity versus temperature and slim hysteresis loops. Furthermore, finite non-zero values of field-induced polarization above the transition temperature are retained.[10]

The ECE also strongly depends on the intensity of the applied electric field following $\Delta T_{EC} \sim E^{2/3}$.[11] Thus, the limiting dielectric strength E_D of ceramic components needs to be increased which is expected to be achieved by reducing the material thickness.[12]

Ferroelectric thin films show high ECE due to their high breakdown field allowing for the application of electric fields around 90 kV mm^{-1}.[3,13] On the other hand, thin films only have a small thermal mass leading to challenges in reliable analysis and limited potential applications.

Multilayer ceramic (MLC) structures allow for the combination of the high thermal mass of a bulk material with a reduced thickness of the single ceramic layers. The effect of MLC design on the ECE has mainly been studied on custom-made $BaTiO_3$ MLCs[14,15] ($\Delta T/\Delta E \sim 0.1 \cdot 10^{-6}$ K m V^{-1}) or on commercially available multilayer ceramic capacitors ($\Delta T/\Delta E \sim 0.02 \cdot 10^{-6}$ up to $0.09 \cdot 10^{-6}$ K m V^{-1}).[16–18]

In this work, we investigate MLC device structures based on PMN-8PT. A ΔT_{EC} of 0.21 K (ΔE = 2.1 kV mm^{-1}; $\Delta T/\Delta E \sim 0.10 \cdot 10^{-6}$ K m V^{-1}) has been measured in our previous work using sheath thermocouple.[19] Recent work by Hirose et al. showed a ΔT_{EC} of 1.2 K (ΔE = 10.3 kV mm^{-1}; $\Delta T/\Delta E \sim 0.12 \cdot 10^{-6}$ K m V^{-1}) directly measured on PMN-10PT MLCs[20] while Fulanovic et al. achieved 2.26 K (ΔE = 10 kV mm^{-1}; $\Delta T/\Delta E \sim 0.23 \cdot 10^{-6}$ K m V^{-1}) for MLCs with the same material composition.[21]

The aim of the here considered investigations is to determine the influence of direct measurement techniques on the ECE of PMN-8PT MLCs. A recent review revealed, that still only 13 % of all published ECE data are measured directly[22] and there are many different methods for direct ECE characterization described in literature[23,24,17,25–27]. The doubts over the reliability of the indirect methods makes paramount the importance of direct measurements. Therefore, we here use four different measurement set-ups on samples from the same batch in order to compare the results obtained by the different methods. Measured data is presented and differences between the measurement methods will be discussed. Moreover, microstructural, dielectric and ferroelectric properties are investigated.

II. EXPERIMENTAL PROCEDURE

The MLC preparation as well as microstructural and electrical characterization can be found in detail elsewhere.[19] The direct electrocaloric temperature change was measured by thermocouple (TC), thermistor (TR), quasi-adiabatic calorimetry (AC), and deduced from differential scanning calorimetry (DSC) direct heat measurement.

For TC measurement, electrode wires and type K thermocouple with a thickness of 25 µm were attached directly to the MLC using Kapton® tape. The pulse time in these measurements was 2.5 s with 0.125 s rise/fall time. Measurement results have been taken under decreasing electric fields. The TC measurement set-up is described in detail elsewhere.[28]

For TR, direct reading of the temperature change due to the application and removal of an electric field was achieved by the attachment of a small bead thermistor (PSB-S9, Shibaura Electronics CO., LTD., *Japan*) on the sample surface. A temperature-controlled chamber ensures isothermal conditions with a temperature stabilization of 0.002 K. Copper wires were glued with silver varnish to the sample for connection with the high voltage source (High Voltage Amplifier 610E, Trek Inc., *USA*). The electric field is applied within a time span of 0.001 s to ensure adiabatic conditions. A detailed description of the measurement set-up can be found elsewhere.[29]

The DSC measurements were performed with an in-house-modified differential scanning calorimeter (DSC 200 F3, Netzsch, *Germany*), as described elsewhere.[30]

Quasi-adiabatic measurements were performed with a custom-built calorimeter under high vacuum-condition (about $1 \cdot 10^{-6}$ mbar). The setup consists of a vacuum bell chamber with two gold-coated copper vacuum chambers inside. The outer copper chamber is used to control the environment temperature. The sample is placed in the inner chamber to ensure a homogenous heat flow from the outside. High voltage is applied to the bottom electrode of the MLC sample. The Kapton®-insulated type K thermocouple is fixed with alumina compound to the top electrode. AC measurements were performed between 26 and 100 °C. Each measurement cycle consists of six dc electric field pulses with duration of 10 s and 30 s intervals inbetween, with magnitudes of 2, 3, and 4 $kV \cdot mm^{-1}$. The voltage pulse is generated by a function signal generator (Model 3390, Keithley, *USA*) and amplified by a high-voltage amplifier (PD05034, Trek, *USA*). The EC temperature change is recorded using a temperature controller (Model 336, Lakeshore Cryotronics, Inc., *USA*). For the AC measurement, temperature change of the participating subsystem ΔT_{EC}, i.e., the part of the MLC sample covered with the electrodes is determined by taking into account the geometry of the system and the heat capacities of its components $\Delta T_{EC} = \Delta T \sum \frac{C_p^i}{C_p^{EC}}$. Here C_p^i represents the heat capacity of each subsystem, which is in contact with the sample (i.e. total MLC sample, conductive silver, alumina glue, copper wires) and Cp^{EC} represents the heat capacity of the MLC sample covered by the electrode (active MLC part).[31] The temperature dependent correction factor used for the AC method was 1.232 to 1.285 in the observed temperature range.

III. RESULTS AND DISCUSSION

Figure 1 shows the microstructure of the sintered MLC samples with a layer thickness of 86 µm (MLC_86; a) and 39 µm (MLC_39; b), respectively. The Ag/Pd electrode layers are about 2 µm thick for all MLC samples. Both samples show a similar porosity Φ around 2.3 %. The grain size distribution is homogeneous and shows values of d_{50} = 1.21 µm (MLC_86) and d_{50} = 1.03 µm (MLC_39).

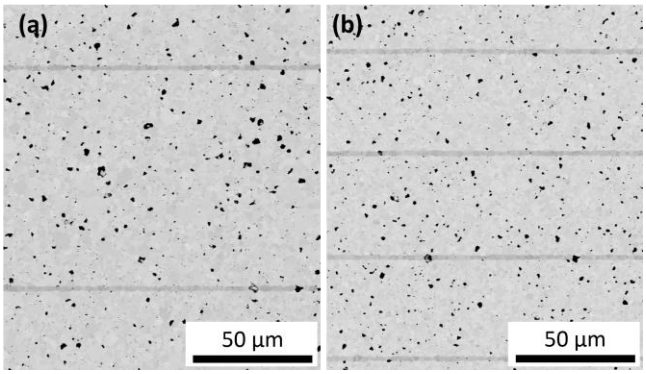

Figure 1: FESEM image of PMN-8PT MLC_86 (a) and MLC_39 (b).

The relative permittivity ε_r and the dielectric loss factor *tan* δ measured in dependence of temperature as well as the ferroelectric hysteresis loops ($P(E)$) measured at room temperature are displayed in Figure 2.

The results show a broad curve progression of ε_r in dependence of temperature with a frequency dependent maximum. It confirms the relaxor behavior of PMN-8PT. The maximum permittivity $\varepsilon_{r,max}$ ~ 21'000 at a temperature of maximum permittivity T_m = 31.3 °C at 1 kHz is comparable to values obtained on undoped PMN-8PT bulk ceramics.[32] The dielectric loss factor *tan* δ at T_m is 0.031. Small deviation of dielectric properties of MLCs are assumed to result from silver migration from the inner electrodes, leading to values analogous to silver doping.[33]

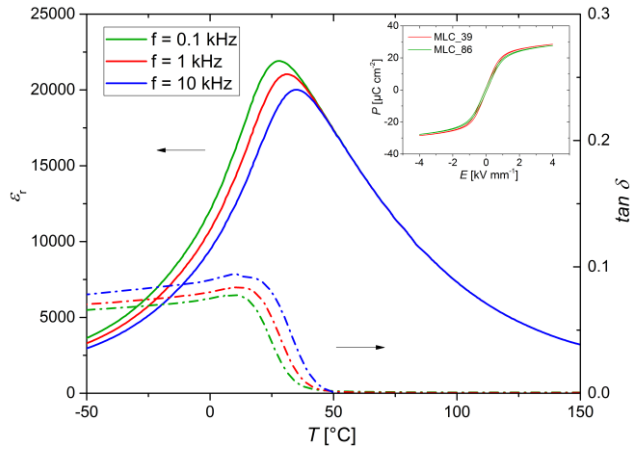

Figure 2: Temperature dependence of relative permittivity ε_r and dielectric loss factor *tan* δ for PMN-8PT MLC_86. (Inset: $P(E)$ hysteresis loops measured at room temperature (f = 5 Hz))

Both $P(E)$ hysteresis loops (Figure 2, inset) show small hysteresis areas. This indicates low ferroelectric losses and is beneficial for the cycling of the EC device structure in a refrigeration system, since it minimizes additional heat generation during cooling application.

The hysteresis loops are only minimally affected by variations of the active layer thickness. Values for remnant polarization P_r = 1.35 µC cm^{-2} and coercive field E_c = 0.06 kV mm^{-1} were measured. The maximum polarization

of P_m = 28.5 µC cm^{-2} is slightly higher for the samples with 39 µm layer thickness, than for the samples with 86 µm layers (P_m = 27.7 µC cm^{-2}). The results of $P(E)$ hysteresis measurements show similar values as for bulk materials.[19] Compared to bulk material, essential improvement could be made in the dielectric strength. The maximum applicable electric field for bulk samples was limited to 7 kV mm^{-1} while the MLC samples could withstand electric fields up to 12 - 16 kV mm^{-1} at room temperature.

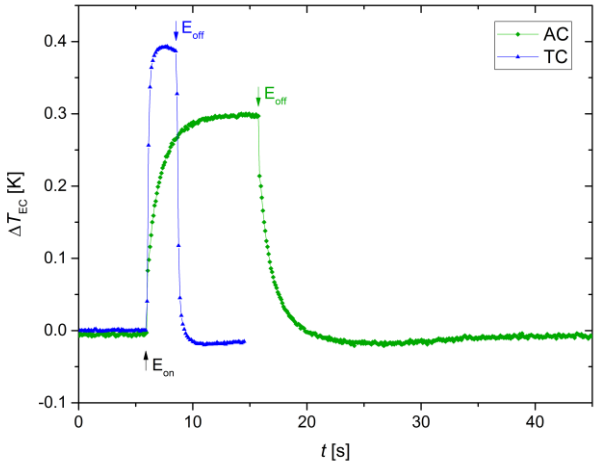

Figure 3: Time dependent electrocaloric response to a 2 kV mm^{-1} electric field at T = 30 °C obtained by AC and TC.

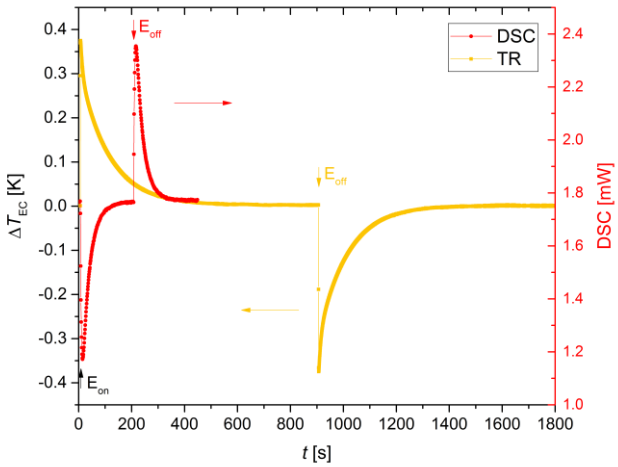

Figure 4: Time dependent electrocaloric response to a 2 kV mm^{-1} electric field at T = 30 °C obtained by DSC and TR.

We already published data on PMN-8PT MLCs based on direct EC measurements performed with a sheath thermocouple ($\Delta T_{EC,max}$ (2.1 kV mm^{-1}) = 0.21 K).[19] They showed a strong deviation from literature and bulk material data deduced from modified DSC ($\Delta T_{EC,max}$ (2 kV mm^{-1}) = 0.58 K).[19,32] The reason for the deviations can be found in the inferior heat transport through the thermocouple casing and thermal losses because of the non-adiabatic measurement set-up.

In order to provide reliable data for ECE properties on MLC samples, different direct measurement set-ups were tested on samples of the same batch. The single measurement values are depicted in Figure 3 and Figure 4. Measurements using thermocouples for direct temperature reading were performed in a short time span. The electric field was applied within 6 s and held for 2 s (TC) and 10 s (AC), respectively. For AC, absence of cooling under the electric field is evidence of the excellent insulation of the measurement set-up. The faster response of the TC measurement is mainly due to the small thermal mass and good thermal connection between sample and temperature sensor.

Single measurements using TR and DSC were carried out in a longer time span, up to 30 min. After application of the electric field, stabilization of the ambient temperature was required. TR measurement also showed a good insulation of the set-up with low thermal losses, which can be deduced from the long external time constant (τ_{ext} = 96 s at T = 30 °C) for heat transfer to the environment. For TR measurement the electric field was held for 900 s while in DSC measurement the electric field was removed after 200 s. For the DSC method, the heat Q was obtained from the areas of exothermal and endothermal peaks, respectively (Q = 0.13 J g^{-1} at ΔE = 2 kV mm^{-1}, T = 30 °C)). The EC temperature change ΔT_{EC} was deduced from the heat data assuming a constant heat capacity of 0.35 J g^{-1} K^{-1}.[34]

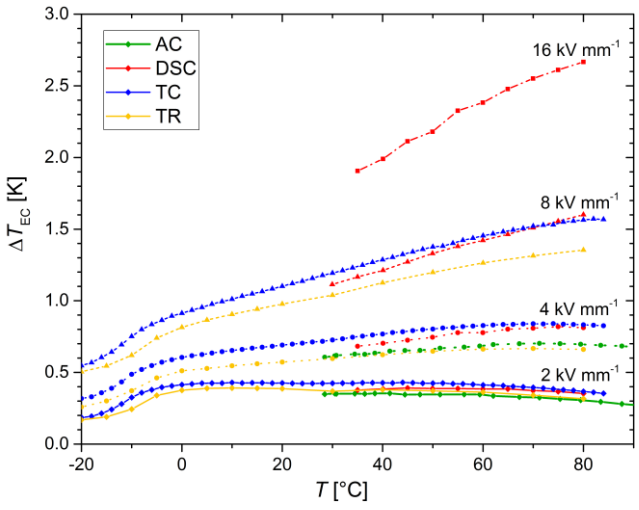

Figure 5: Comparison of EC temperature change ΔT_{EC} of MLC_86 measured with different set-ups and different electric fields in dependence of temperature T.

Figure 5 shows the results of the temperature and electric field dependent ECE obtained from the different measurement set-ups for MLCs with 9 layers of 86 µm thickness. They show good agreement of ΔT_{EC} ~ 0.4 K at 2 kV mm^{-1}($\Delta T/\Delta E$ = 0.2·10^{-6} m K V^{-1}). With increasing electric field, the results from TR and AC measurements are slightly lower compared to data from DSC and TC measurements which both show good agreement

independent of the applied electric field. At 8 kV·mm^{-1} we observed a maximum ΔT_{EC} of 1.6 K around 80 °C (DSC, TC), but only 1.4 K with the TR set-up. Since all samples were taken from the same batch, the reason for this deviation could be an inferior heat transfer from the sample to the TR due to the glass insulating layer of the thermistor bead. Lower values from AC measurement can also be explained by an additional layer between the thermocouple and the sample surface. Here, the alumina glue, used to fix the thermocouple, disables direct contact to the sample and thus hampers the heat transfer. The AC temperature change of the participating subsystem ΔT_{EC}, i.e., the part of the MLC sample covered with the electrodes is determined by taking into account the geometry of the system and the heat capacities of its components as described by Rožič et al.[31]

A compilation of advantages and shortcomings of the different utilized characterization methods can be found in **Fehler! Verweisquelle konnte nicht gefunden werden.**, which also shows specific characteristics like measurement temperature range T_{meas}, response time t_{res}, and temperature resolution R_T. For TC measurement fast response times were achieved by using a thermocouple with a small thermal mass. Hence, short electric field pulses were used and combined with relatively long rise/fall times to prevent the samples from damage. Similar time spans were employed using the AC measurement. The set-up showed a good thermal insulation, but due to the additional alumina layer between the thermocouple and the sample the heat transfer is hindered. The isothermal DSC measurement allows for sensitive detection of enthalpy changes and good temperature resolution but since it is only a quasi-direct method, the temperature and field dependent heat capacity would be needed to determine the EC temperature change appropriately. Furthermore, the commercial DSC is expensive and has to be modified to allow for the application of electric field to the sample. TR measurement, utilizing a high resolution calorimeter, and DSC both require large time spans to stabilize the measurement temperature. The resulting long electric field pulses, which can be reduced for TR method, could cause additional damage to the sample at higher electric fields.[1] For both, TR and TC measurement, significant corrections become necessary with increasing inactive volume of the set-up. That means if the influence of electrical contacts, temperature sensors or inactive material becomes large compared to the active EC material (e.g. for thin films).

Table 1: Comparison of different ECE characterization methods.

	Advantages	Shortcomings
TC T_{meas}: 77 – 573 K t_{res}: 500 -1000 ms R_T: ± 1 mK	+ Direct temperature measurement + Fast response time + easy to set-up + short time measurement	- With increasing inactive volume, significant corrections become necessary - Sample breakdown can lead to set-up damage
AC (quasi-adiabatic) T_{meas}: 260 – 435 K t_{res}: 1000 ms	+ Direct temperature measurement + Good insulation of the calorimeter + Short time measurement	- Slow response time - Poor thermal contact between thermocouple and sample - Corrections necessary

R_T: ± 10 mK		- Complicated set-up
DSC (isothermal) T_{meas}: 77 - 443 K t_{res}: 1000 ms R_T: < 100 mK	+ High sensitivity by detecting enthalpy changes[1] + Good insulation of the calorimeter	- Quasi direct method - Additional measurement of c_p (E,T) needed - Slow response time - Expensive setup with modifications - Long time measurements - Limited lateral sample dimensions
TR T_{meas}: 77 – 450 K t_{res}: 600 ms R_T: up to ± 2 mK	+ Direct temperature measurement + Fast response time + Easy to set-up + Temperature stabilization ~ 2 mK	- With increasing inactive volume, significant corrections become necessary - Long time measurements (can be reduced if necessary)

Overall, the different metrologies for direct measurement of the ECE of MLC structures reveal a very good agreement and almost double values compared to measurements using sheath thermocouple.[19]

The highest ΔT_{EC} of 2.7 K was deduced by DSC at 80 °C and 16 kV mm^{-1} ($\Delta T/\Delta E$ = 0.17·10^{-6} K m V^{-1}), which is comparable with the literature.[20,21]

The field dependence of ECE at 80 °C is shown in Figure 6. The $\Delta T \sim \Delta E^{2/3}$ dependence at high electric fields published by Lu et al.[11] could be confirmed for PMN-8PT MLCs with the different measurement set-ups.

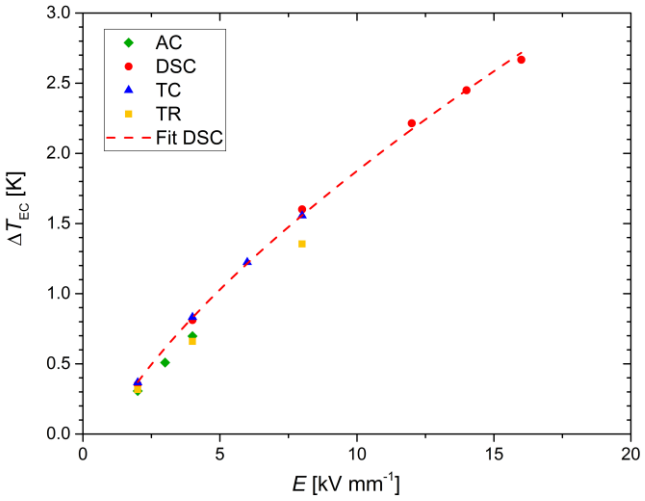

Figure 6: Comparison of EC temperature change ΔT_{EC} of MLC_86 measured with different set-ups at 80 °C in dependence of electric field E.

The temperature dependent ECE measurement at different electric fields (Figure 7) was taken from the TC measurement of MLC_39 samples. The curve progression is similar to results found in PMN-PT bulk ceramics.[7] At low electric fields, ECE shows a peak in the vicinity of the characteristic depolarization temperature T_d. An increase of the applied electric field leads to formation of another, broader peak which shifts towards higher

temperatures as the electric field increases. This second peak appears to be typical for relaxor ferroelectrics due to polar nanoregions[35,36] or it could be a more universal property of ferroelectrics in the supercritical regime.[37]

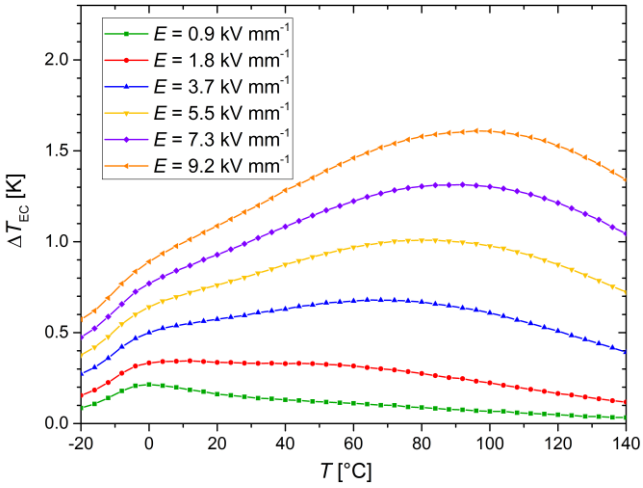

Figure 7: EC temperature change ΔT_{EC} in dependence of temperature T and electric field E for MLC_39.

The influence of the layer thickness on the ECE was investigated by DSC measurements. As can be seen in Figure 8, the EC temperature change is independent of the layer thickness and thus the overall sample thickness in the examined temperature and electric field range. The main difference between MLC_39 and MLC_86 is the electric voltage necessary to generate the electric field and thus the EC temperature change. To reach a ΔT_{EC} of 1.6 K, only 312 V were applied for the MLC_39 samples, while for MLC_86 samples 688 V were necessary. The good agreement between samples of different thicknesses confirms that the highest ECE measured in this study, ΔT_{EC} =2.7 K, could be obtained in MLC_39 by applying voltage values under 1 kV (ΔU ~ 600 V).

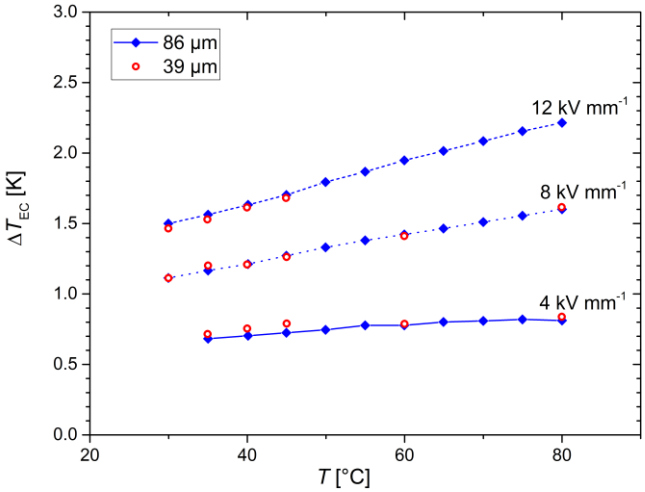

Figure 8: Comparison of temperature T and electric field dependent EC temperature change ΔT_{EC} in dependence of layer thickness.

IV. CONCLUSION

Two different MLC structures consisting of nine ceramic layers of 86 µm and 39 µm thickness have been manufactured successfully. Both samples show a similar porosity Φ ~ 2.3 % and a homogeneous grain size distribution. The dielectric and ferroelectric properties show similar values compared to data measured on bulk materials of the same composition.

Different metrologies were used and compared to test the reliability of direct ECE measurements. All measurement set-ups reveal a good correlation of the EC temperature change as function of both temperature and applied electric field. The best match was obtained using DSC and thermocouple (TC) measurements. Thermistor (TR) or the adiabatic calorimeter (AC) set-up revealed slightly lower ΔT_{EC} values under high electric fields. For the DSC measurements a field independent heat capacity was assumed. Investigation of the dependence of the heat capacity with the external electric field will be required in future research. The temperature and electric field dependent behavior of multilayer ceramic structures was found comparable to bulk material for the investigated PMN-8PT composition. The EC response is found to be independent of the single layer thickness in the studied range, but the decreased thickness compared to bulk material allows for application of higher electric fields with simultaneous decrease of the applied voltage to only a few hundreds of Volts. Under the considered conditions we measured an EC temperature change of 2.7 K under the application of an external electric field of 16 kV mm^{-1} (ΔU ~ 1400 V). These excellent values confirm the significant potential of multilayer relaxor ferroelectrics for energy efficient solid-state cooling and can enable the development of an efficient heat pump technology. The ability of achieving them at common technological voltages will be key to the device success.

V. ACKNOWLEDGEMENT

This work was partly supported by the German Research Foundation (DFG) in context of the priority program Ferroic Cooling (SPP1599).

VI. REFERENCES

[1]T. M. Correia and Q. Zhang, "*Electrocaloric Materials*, Springer-Verlag, Berlin, Heidelberg (2014).

[2]P. Kobeko and J. Kurtschatov, "*Dielektrische Eigenschaften der Seignettesalzkristalle," Z. Phys.* **66,** 192–205 (1930).

[3]A. S. Mischenko, Q. Zhang, J. F. Scott, R. W. Whatmore and N. D. Mathur, "*Giant Electrocaloric Effect in Thin-Film $PbZr_{0.95}Ti_{0.05}O_3$,*" Science **311,** 1270–1271 (2006).

[4]X. Moya, S. Kar-Narayan and N. D. Mathur, "*Caloric materials near ferroic phase transitions," Nat. Mater.* **13,** 439–450 (2014).

[5]D. Saranya, A. Chaudhuri, J. Parui and S. Krupanidhi, "*Electrocaloric effect of PMN-PT thin films near morphotropic phase boundary," Bull. Mater. Sci.* **32,** 259–262 (2009).

[6]R. Chukka, J. W. Cheah, Z. Chen, P. Yang, S. Shannigrahi, J. Wang and L. Chen, "*Enhanced cooling capacities of ferroelectric materials at morphotropic phase boundaries," Appl. Phys. Lett.* **98,** 242902 (2011).

[7]J. Peräntie, H. N. Tailor, J. Hagberg, H. Jantunen and Z.-G. Ye, "*Electrocaloric properties in relaxor ferroelectric* $(1-x)Pb(Mg_{1/3}Nb_{2/3})O_3–xPbTiO_3$ *system," J. Appl. Phys.* **114,** 174105 (2013).

[8]L. Shebanovs, K. Borman, W. N. Lawless and A. Kalvane, "*Electrocaloric Effect in Some Perovskite Ferroelectric Ceramics and Multilayer Capacitors," Ferroelectrics* **273,** 137–142 (2002).

[9]M. Vrabelj, H. Uršič, Z. Kutnjak, B. Rožič, S. Drnovšek, A. Benčan, V. Bobnar and L. Fulanović, et al., "*Large electrocaloric effect in grain-size-engineered 0.9Pb(Mg1/3Nb2/3)O3–0.1PbTiO3," J. Eur. Ceram. Soc.* **36,** 75–80 (2016).

[10]G. A. Samara, "*The relaxational properties of compositionally disordered* ABO_3 *perovskites," J. Phys.: Condens. Matter* **15,** R367 (2003).

[11]S. G. Lu, Z. H. Cai, Y. X. Ouyang, Y. M. Deng, S. J. Zhang and Q. Zhang, "*Electrical field dependence of electrocaloric effect in relaxor ferroelectrics," Ceram. Int.* **41,** S15-S18 (2015).

[12]C. Neusel and G. A. Schneider, "*Size-dependence of the dielectric breakdown strength from nano- to millimeter scale," J. Mech. Phys. Solids* **63,** 201–213 (2014).

[13]A. S. Mischenko, Q. Zhang, R. W. Whatmore, J. F. Scott and N. D. Mathur, "*Giant electrocaloric effect in the thin film relaxor ferroelectric* $0.9\ PbMg_{1/3}Nb_{2/3}O_3$*-*$0.1\ PbTiO_3$ *near room temperature," Appl. Phys. Lett.* **89,** 242912 (2006).

[14]Y. Bai, G. Zheng and S. Shi, "*Direct measurement of giant electrocaloric effect in BaTiO3 multilayer thick film structure beyond theoretical prediction," Applied Physics Letters* **96,** 192902 (2010).

[15]Y. Bai, G.-P. Zheng, K. Ding, L.-J. Qiao, S.-Q. Shi and D. Guo, "*The giant electrocaloric effect and high effective cooling power near room temperature for $BaTiO_3$ thick film," J. Appl. Phys.* **110,** 94103 (2011).

[16]S. Kar-Narayan and N. D. Mathur, "*Direct and indirect electrocaloric measurements using multilayer capacitors," J. Phys. D: Appl. Phys.* **43,** 32002 (2010).

[17]S. Kar-Narayan, S. Crossley, X. Moya, V. Kovacova, J. Abergel, A. Bontempi, N. Baier and E. Defay, et al., "*Direct electrocaloric measurements of a multilayer capacitor using scanning thermal microscopy and infra-red imaging," Appl. Phys. Lett.* **102,** 32903 (2013).

[18]K. Ding and G.-P. Zheng, "*Scaling for the refrigeration effects in lead-free barium titanate based ferroelectric ceramics," Journal of Electroceramics* **32,** 169–174 (2014).

[19]C. Molin and S. Gebhardt, "*PMN-8PT device structures for electrocaloric cooling applications," Ferroelectrics* **498,** 111–119 (2016).

[20]S. Hirose, T. Usui, S. Crossley, B. Nair, A. Ando, X. Moya and N. D. Mathur, "*Progress on electrocaloric multilayer ceramic capacitor development," APL Mater.* **4,** 64105 (2016).

[21]L. Fulanović, S. Drnovšek, H. Uršič, M. Vrabelj, D. Kuščer, K. Makarovič, V. Bobnar and Z. Kutnjak, et al., "*Multilayer 0.9Pb(Mg1/3Nb2/3)O3–0.1PbTiO3 elements for electrocaloric cooling," Journal of the European Ceramic Society* **37,** 599–603 (2017).

[22]Y. Liu, J. F. Scott and B. Dkhil, "*Direct and indirect measurements on electrocaloric effect: Recent developments and perspectives," Applied Physics Reviews* **3,** 31102 (2016).

[23]S. Crossley, T. Usui, B. Nair, S. Kar-Narayan, X. Moya, S. Hirose, A. Ando and N. D. Mathur, "*Direct electrocaloric measurement of $0.9Pb(Mg_{1/3}Nb_{2/3})O_3$-$0.1PbTiO_3$ films using scanning thermal microscopy," Appl. Phys. Lett.* **108,** 32902 (2016).

[24]J. Hagberg, A. Uusimaki and H. Jantunen, "*Electrocaloric characteristics in reactive sintered 0.87 $Pb(Mg_{1/3}Nb_{2/3})O_3$-0.13 $PbTiO_3$*," Appl. Phys. Lett. **92,** 132909 (2008).

[25]J. Koruza, B. Rožič, G. Cordoyiannis, B. Malič and Z. Kutnjak, "*Large electrocaloric effect in lead-free $K_{0.5}Na_{0.5}NbO_3$-$SrTiO_3$ ceramics," Appl. Phys. Lett.* **106,** 202905 (2015).

[26]B. Rožič, H. Uršič, J. Holc, M. Kosec and Z. Kutnjak, "*Direct Measurements of the Electrocaloric Effect In Substrate-Free PMN-0.35pt Thick Films on a Platinum Layer," Integr. Ferroelectr.* **140,** 161–165 (2012).

[27]M. Sanlialp, V. V. Shvartsman, M. Acosta, B. Dkhil and D. C. Lupascu, "*Strong electrocaloric effect in lead-free $0.65Ba(Zr_{0.2}Ti_{0.8})O_3$-$0.35(Ba_{0.7}Ca_{0.3})TiO_3$ ceramics obtained by direct measurements," Appl. Phys. Lett.* **106,** 62901 (2015).

[28]J. Peräntie, J. Hagberg, A. Uusimaki and H. Jantunen, "*Electric-field-induced dielectric and temperature changes in a ‹011›-oriented $Pb(Mg_{1/3}Nb_{2/3})O_3$-$PbTiO_3$ single crystal," Phys. Rev. B* **82,** 134119 (2010).

[29]Z. Kutnjak, B. Rožič, R. Pirc and J. G. Webster, "*Electrocaloric Effect: Theory, Measurements, and Applications*, in Wiley Encyclopedia of Electrical and Electronics Engineering (2015).

[30]F. Le Goupil, A. Berenov, A.-K. Axelsson, M. Valant and N. M. Alford, "*Direct and indirect electrocaloric measurements on -$PbMg_{1/3}Nb_{2/3}O_3$-30$PbTiO_3$ single crystals ," J. Appl. Phys.* **111,** 124109 (2012).

[31]B. Rožič, B. Malič, H. Uršič, J. Holc, M. Kosec, B. Neese, Q. Zhang and Z. Kutnjak, "*Direct Measurements of the Giant Electrocaloric Effect in Soft and Solid Ferroelectric Materials," Ferroelectrics* **405,** 26–31 (2010).

[32]C. Molin, M. Sanlialp, V. V. Shvartsman, D. C. Lupascu, P. Neumeister, A. Schönecker and S. Gebhardt, "*Effect of dopants on the electrocaloric effect of 0.92 $Pb(Mg_{1/3}Nb_{2/3})O_3$–0.08 $PbTiO_3$ ceramics," J. Eur. Ceram. Soc.* **35,** 2065–2071 (2015).

[33]Y. Sato, H. Kanai and Y. Yamashita, "*Effects of Silver and Palladium Doping on the Dielectric Properties of 0.9Pb(Mg1/3Nb2/3)O3–0.1 PbTiO3 Ceramic," J. Am. Ceram. Soc.* **79,** 261–265 (1996).

[34]H. Uršič, M. Vrabelj, L. Fulanović, A. Bradeško, S. Drnovšek and B. Malič, "*Specific heat capacity and thermal conductivity of the electrocaloric (1-x)Pb($Mg_{1/3}Nb_{2/3}$)O_3–x$PbTiO_3$ ceramics between room temperature and 300°C," Informacije Midem* **45,** 260–265 (2015).

[35]L. J. Dunne, M. Valant, A.-K. Axelsson, G. Manos and N. M. Alford, "*Statistical mechanical lattice model of the dual-peak electrocaloric effect in ferroelectric relaxors and the role of pressure," J. Phys. D: Appl. Phys.* **44,** 375404 (2011).

[36]F. Le Goupil, A.-K. Axelsson, L. J. Dunne, M. Valant, G. Manos, T. Lukasiewicz, J. Dec and A. Berenov, et al., "*Anisotropy of the Electrocaloric Effect in Lead-Free Relaxor Ferroelectrics," Adv. Energy Mater.* **4,** 1301688 (2014).

[37]G. G. Guzmán-Verri and P. B. Littlewood, "*Why is the electrocaloric effect so small in ferroelectrics?," APL Mater.* **4,** 64106 (2016).